NEW DIRECTIONS IN THE QUEST FOR UNALTERED CI-LIKE MATERIAL FROM THE EARLY SOLAR SYSTEM. C. A. Goodrich[1], N. T. Kita[2], M. Zhang[2], P. Mane[1], J. Han[3], T. M. Erickson[4], and V. E. Hamilton[5]. [1]Lunar and Planetary Institute, USRA, 3600 Bay Area Blvd., Houston, TX 77058 USA (goodrich@lpi.usra.edu). [2]WiscSIMS, Dept. of Geoscience, University of Wisconsin-Madison, Madison,Wisconsin 53706, USA. [3]Dept. of Earth and Atmospheric Sciences, University of Houston, Houston, TX 77204 USA. [4]Jacobs/JETS, JSC, Houston, TX 77058 USA. [5]Southwest Research Institute, Boulder, CO 80302 USA.

Introduction: CI meteorites have bulk chemical compositions closely matching the solar photosphere (except volatiles) and thus are considered to represent the starting composition of the Solar System. The return of CI-like samples from asteroid (162173) Ryugu by Hayabusa2 has greatly bolstered studies of CI [1-3]. However, both CI and the Ryugu samples are CI1, i.e., they were extensively altered by aqueous fluids on their parent bodies so the mineralogy, textures, and oxygen isotope compositions of their CI3 precursors have been obscured. Fortunately, they contain rare remnants of primordial minerals in the form of small anhydrous silicate and Ca-Al-rich grains, and detailed petrologic and isotopic studies of these grains have helped elucidate the nature of their precursors [4-12]. Here, we continue our work [13] on petrologic and isotopic studies of such phases in Ryugu particle C0137.

In addition, we are mining a rich source of CI-like materials that occur as xenoliths in polymict ureilites. These xenoliths were implanted into regolith on ureilitic asteroids ~10-50 Myr after CAI [14,15], and may represent CC bodies that are not being sampled by independent meteorites on Earth [16,17]. Here we describe several unique types of C2 xenoliths that may give a new view into the nature of CI3 materials.

Samples and Methods: We studied a polished mount [13] of Ryugu particle C0137 (~2.3 mm^2 of exposed sample) and polished sections of polymict ureilites Northwest Africa (NWA) 10657 (5 sections) and Dar al Gani (DaG) 165. Scanning electron microscope (SEM) observations were carried out using the Phenom XL (LPI) and the Zeiss EVO (UMass). Electron microprobe (EMPA) data were obtained using the JEOL 8530 FE (ARES/JSC) and Cameca SXFIVE-Tactis (UMass). The Ryugu section was mapped with individual, slightly overlapping, X-ray maps of 141×141 or 153×153 μm at 1024×1024 pixels and dwell times of 2 to 5 ms. Maps were processed in ImageJ [18] and XMapTools [19]. Cathodoluminescene (CL) observations were made on ten MgO-rich olivine grains in C0137 using a JEOL 7900F FE-SEM (ARES/JSC) equipped with a Gatan Monarc CL detector.

Oxygen isotope analyses of a large grain of Fo_{59} in C0137 (Fig. 1) and a grain of Fo_{76} in clast 25 of NWA 10657_001 (Fig. 2a) were obtained by IMS 1280 at WiscSIMS with a beam size of 3 μm and analytical settings similar to [20]. Fo_{100-59} standards were used to calibrate the instrumental biases. The external reproducibility (2SD) of running standard olivine was 0.7‰ for $\delta^{18}O$ and ~1.0‰ for $\delta^{17}O$ and $\Delta^{17}O$.

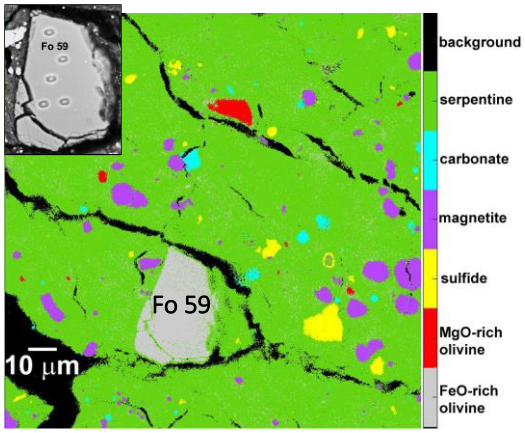

Fig. 1. Mineral classification map created in XMapTools from combined Mg, Fe, Si, Ca, S, and C X-ray maps of olivine-bearing area of Ryugu C0137. Fo 98-99 olivines are bright red. Fo 59 olivine grain was analyzed by SIMS (inset).

Results: X-ray mapping of C0137 revealed olivine grains only in one contiguous area of ~0.23 mm^2. This area does not appear to be a discrete clast. Most olivine grains are <10 μm in size and MgO-rich (Fo_{98-99}), but one ~25×35 μm-sized grain of FeO-rich (Fo_{59}) olivine was observed (Fig. 1). The modal abundance of MgO-rich olivine from 15 mineral classification maps of this area varied from 0.07 to 1.8 area % (avg. ~0.6 area %). The abundance of FeO-rich olivine is ~0.5 area %. The abundance of olivine in the whole section is <0.1 area%.

CI-like xenoliths in polymict ureilites include a variety of types, but none are identical to CI or Ryugu samples [14, 21-25]. We have identified two common C2 types of interest to this study. One type has generally CI-like mineralogy but higher abundances of AOA and CAI-like phases, as well as chondrule remnants and isolated olivine grains, compared with most samples of CI or Ryugu. NWA 10657_001 clast 25 [13] is one of these (Fig. 2a). The other common type has a fine-grained clastic matrix (Fig. 2b) of abundant tiny anhydrous silicate grains (broad-beam EMPA gives higher analytical totals than fully hydrated materials), plus larger olivine and pyroxene grains (olivine of Fo_{99-58}, pyroxene of Mg_{98-85} and $Wo_{0.5-35}$). Clast 37 In DaG 165 [13] is one of these types. We are conducting oxygen isotope mapping (NanoSIMS), FIB/TEM and μ-FTIR studies of xenoliths of both types.

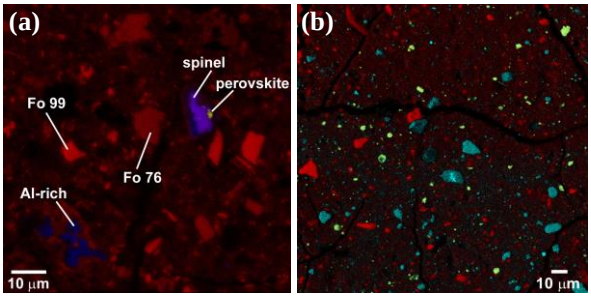

Fig. 2. Combined element X-ray maps. (a) Clast 25 in NWA 10657_001. Mg = red, Al = blue, Ti = yellow. Red grains of various intensities are olivines of different compositions. Fo_{76} grain was analyzed for oxygen isotopes. (b) Clast 5 in NWA 10657_006. Mg = red, Fe = cyan, S = yellow. This clast has a clastic matrix of abundant fine olivine and pyroxene grains.

Minor element (Cr, Mn, Ca) abundances of olivine grains in Ryugu C0137 and several xenoliths are consistent with those in other samples of Ryugu and CI [4-12]. Inferred AOAs are consistent with compositions argued by [9] to be AOA-like rather than chondrule-like. We observed high CL intensity in forsterite grains in C0137, but no zoning such as that in chondrule olivines [26]. The grains may be smaller than the scale of zonation, but further work is needed to test this.

Oxygen isotope ratios for the analyzed olivines plot near the CCAM line with $\Delta^{17}O = -2.0 \pm 0.6$‰ (2SE, n=5) for the Fo_{59} grain in Ryugu and -3.1 ± 0.9‰ (2SE, n=1) for the Fo_{76} grain in NWA 10657_001 clast 25 (Fig. 3).

Discussion: Our results for Ryugu C0137 are similar to those of others for Ryugu samples in showing very low abundances of anhydrous silicates and CAI-like phases [1-10], and confirm that these grains can occur dispersed through matrix and are not limited to obvious clasts [e.g., 10]. In these respects, Ryugu is similar to CIs. [4,10] found that anhydrous primary minerals in Ryugu and CI exhibit a bimodal distribution of oxygen isotope compositions: ^{16}O-rich (refractory) and ^{16}O-poor (chondrule-like). [10] noted that the abundance ratio of ^{16}O-rich to ^{16}O-poor primary materials was similar to that of comet 81P/Wild 2, but also found that the $\Delta^{17}O$ values of the ^{16}O-poor grains were like those of chondrules in CO, CM, and CV. The $\Delta^{17}O$ of –2.0‰ from the Fo_{59} grain studied here further supports a similarity to chondrules in CO, CM, and CV [10], rather than CR or cometary material (Fig. 3).

The CI-like xenolith populations in polymict ureilites are different from Ryugu and CI and could provide new insights into CI3 materials. The clastic-textured xenoliths (Fig. 2b) are intriguing because they have C2-like abundances of primary minerals but do not show chondritic textures such as other "CI-like" chondrites (e.g.,Tagish Lake, Tarda).

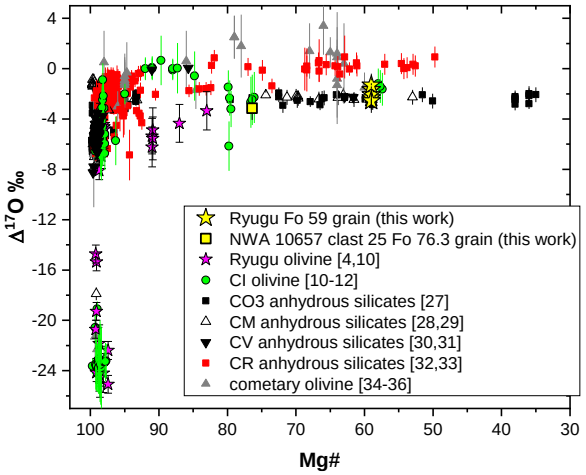

Fig. 3. Oxygen isotope compositions ($\Delta^{17}O$) of analyzed FeO-rich olivine grains compared with anhydrous silicates in other Ryugu samples, CI, CO, CM, CV, CR, and cometary samples.

References: [1] Nakamura E. et al. (2022) *Proc. Japanese Acad., Ser. B 98*, 227-282. [2] Nakamura T. et al. (2022) *Science*, 10.1126/science.abn8671. [3] Ito M. et al. (2022) *Nat. Astr.*, doi.org/10.1038/s41550-022-01745-5. [4] Liu M-C. et al. (2022) *Nat. Astr.*, doi.org/10.1038/s41550-022-01762-4. [5] Mikouchi T. et al. (2022) *LPSC 53*, #1935. [6] Mikouchi T. et al (2022) *85th MSM*, #6180. [7] Nakashima D. et al. (2022) *Hayabusa Symposium*. [8] Ando T. et al. (2022) *13th NIPR Symposium*. [9] Mikouchi T. et al. (2023) *86th MSM*, #6178. [10] Kawasaki N. et al. (2022) *Sci. Adv.* 8, eade2067. [11] Morin G. L. F. et al. (2022) *GCA 332*, 203-219. [12] Piralla M. et al. (2020) *GCA* 269, 451-464. [13] Goodrich C.A. et al. (2023) *LPSC* 54, #1446. [14] Goodrich C.A. et al. (2021) *Planet. Sci. Jour.* 2:13 (15pp), 2121 February. [15] Bischoff A. et al. (2022) *M&PS* 57, 1339-1364. [16] Goodrich C.A. (2023) *85th MSM*, #6166. [17] Russell S. et al. (2022) *M&PS* 57, 277-301. [18] Schneider C. et al. (2012) *Nature Methods* 9, 671-675. [19] Lanari P. et al. (2014) *Computers & Geoscience*, 62, 227-240. [20] Ushikubo T. et al. (2017) *GCA* 201, 103-122. [21] Goodrich C.A. et al. (2019) *LPSC* 50, #1312. [22] Brearley A. J. & Prinz M. (1992) *GCA* 56, 1373-1386. [23] Patzek M. et al. (2018) *M&PS* 53, 2519-2540. [24] Patzek M. et al. (2018) *81st MSM*, #6183. [25] Goodrich C. A. et al. (2019) *M&PS* 54, 2769-2813. [26] Libourel G. and Portail M. (2018) *Sci. Adv.* 2018;4: eaar3321. [27] Tenner T. J. et al. (2013) *GCA* 102, 226-245. [28] Chaumard N. et al. (2018) *GCA* 228, 220-242. [29] Chaumard et al. (2021) *GCA* 299, 199-218. [30] Hertwig A. T. et al. (2018) *GCA* 224, 116-131. [31] Hertwig A.T. et al. (2019) *M&PS* 54, 2666-2685. [32] Schrader D. L. et al. (2013) *GCA* 101, 302-327. [33] Tenner T. J. et al. (2015) *GCA* 148, 228-250. [34] Nakashima D. et al. (2012) *EPSL* 357, 355-365. [35] Defouilloy C. et al. (2017) *EPSL* 465, 145-154. [36] Ogliore R. C. et al. (2015) *GCA* 166, 74-91.